Chapter 5
FEC Scheme II in the DLC Protocol of Wireless ATM

This chapter applies punctured Turbo code schemes to protect the header and various payloads of wireless ATM cell by the combination of programmable interleaving and puncturing. Their performance is analyzed for the Rayleigh fading channel and show more significant reduction in CLR than the other FEC schemes. The proposals also provide the good balance designs for CLR and payload BER, and offer the potential for future evolutionary improvement of wireless ATM coding schemes.

5.1 Turbo Codes

As a new class of convolutional codes, Turbo code was presented in 1993 [10]. The term "Turbo code" is given for its iterative decoding scheme with reference to the Turbo engine principle. This code has recently attracted a great deal of attention because of its outstanding performance and reasonable decoding complexity so as to be widely applied to various wireless systems [52]–[55]. Having obtained better results using convolutional codes, it is expected to realize much better performance of wireless ATM by using Turbo codes.

Turbo code is a novel class of parallel concatenated recursive systematic codes [56], which is a linear block code in fact. Figure 5.1 shows the block diagram of a two dimensional Turbo encoder, where the component encoder is always a recursive systematic convolutional (RSC) encoder with feedback due to its better performance than the equivalent nonsystematic convolutional code at any SNR, for code rates larger than 2/3 [57]. It is also better than the non-recursive systematic convolutional code when the interleaver is used [58]. As the most distinctive feature of the Turbo encoder, the interleaver is between the component encoders, whose main purpose is to distribute uniformly the error correction capability over all information bits so that after the correction in one dimension the remaining errors should become correctable error patterns in the second dimension. Generally, there is a puncturer in the output of the encoder to obtain a desired rate by puncturing appropriate encode bits. Its

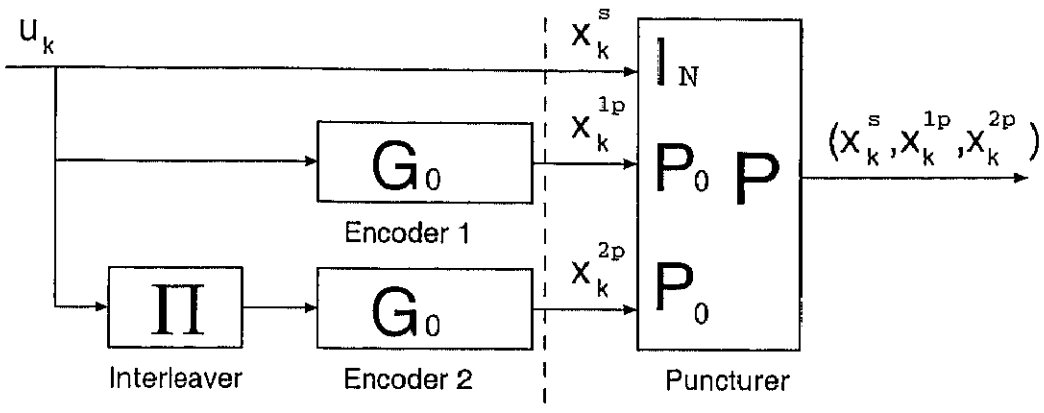

Figure 5.1: Two dimensional frame-based Turbo encoder

role is identical to that of the convolutional code counterpart. Sometimes, this Turbo code with puncturer is called the punctured Turbo code (PTC).

The encoder first breaks the input sequence into $(N-t)$ bit information blocks. Let one of information blocks be $\mathbf{u} = (u_1, u_2, ..., u_{N-t})$, where u_k is an information bit, and t is the number of symbols needed for the trellis termination. In general, t is equal to the memory of the component encoder, i.e., K-1, K is its constraint length. One tail generally terminates only one RSC encoder to the zero state. But when an available interleaver is applied, only one tail is sufficient to drive two component encoders to the zero state after encoding both the straight and the interleaved sequences of information bits [59]. The process of interleaving data sequence can be regarded as a permutation of bit positions in an input packet. If the original index position is denoted as l and the permuted index as $\tilde{l} = \alpha(l)$, then the interleaver must have the property that

$$\forall l. \qquad \tilde{l} = l \mod p, \tag{5.1}$$

where p is the sequence maximal length of the feedback primitive polynomial of degree $K-1$ ($p = 2^{K-1} - 1$). By designing interleavers that satisfy the above condition, the two encoders are guaranteed to end in the same final state [60]. Therefore, only the first RSC encoder is necessarily terminated to the zero state by one tail.

After appended t bits, each N bit block is encoded twice but in a different order. $X^{1p} = (x_1^{1p}, x_2^{1p}, ..., x_N^{1p})$ and $X^{2p} = (x_1^{2p}, x_2^{2p}, ..., x_N^{2p})$ represent the parity words generated by each component encoder, $X^s = (x_1^s, x_2^s, ..., x_N^s)$ is its information word.

Without any essential loss of generality, two component codes are assumed to be identical. Let $G_c = [I_N|G_0]$ be the systematic generator matrix for two same component RSC encoders of rate $1/n$ by the trellis termination at all, where I_N is

an $N \times N$ identity matrix, G_0 is $N \times \mathrm{r}_0$ parity check part of G_c, and r_0 is the length of the redundancy vector. An interleaver of length N is described by an $N \times N$ permutation matrix $\prod$, which contains a single "1" in each row and column. The shorthand notation of the matrix $\prod$ is $(i_1, i_2, \ldots, i_N)$, where the integer i_j indicates the position of the "1"element in the j-th column of $\prod$. The interleaver structure affects the distance property of the resulting Turbo code. So the type and size of the interleaver play essential roles in determining its performance.

Because the best performance is obtained when encoded bits at the systematic positions of encoded bits are not punctured [10], a puncturing matrix P takes the block-diagonal form of $[I_N|P_0|P_0]$, where P_0 is the puncturing matrix of size $\mathrm{r}_0 \times \mathrm{r}_1$ (r_1 is the length of a redundancy vector after being punctured). Then, the generator matrix of the Turbo code is:

$$G = [I_N|G_0|\prod G_0]P = [I_N|G_0P_0|\prod G_0P_0]. \tag{5.2}$$

The codeword corresponding to an encoder input frame $\mathbf{u}$ is:

$$X = [\mathrm{x}_k^s|\mathrm{x}_k^{1p}|\mathrm{x}_k^{2p}] = [\mathrm{u}|\mathrm{u}G_0P_0|\mathrm{u}\prod G_0P_0]. \tag{5.3}$$

where, x_k^{1p} and x_k^{2p} are the two redundancy vectors of length r_1, respectively.

The rate of Turbo code G is :

$$R = \frac{N-t}{2|\mathrm{r}_1| + N} = \frac{N-t}{2w(P_0) + N}. \tag{5.4}$$

Here, $w()$ denotes the Hamming weight. Since the information sequence is divided into blocks of a certain length $(N-t)$, the Turbo code is usually considered as a kind of $(2|\mathrm{r}_1| + N, N-t)$ block codes that start and end at the zero states of both RSC codes [58].

If the same component encoders have a rate of $\frac{1}{n}$, Turbo encoder outputs $(2n-1)$ symbols for each input symbol when puncturing is ignored. After puncturing, the encoding rate R (local rate) satisfies:

$$\frac{1}{2n-1} \leq R \leq 1. \tag{5.5}$$

5.2 RCPT Code with UEP

Turbo codes can also provide UEP in a natural way. For example, changing the interleaver size can influence BER [58]. But this method would be cumbersome from the viewpoint of the hardware implementation. Another option is to apply the different encoding rates, which can be realized by using the same component code, the available interleaver and the different puncturing matrices [61]. This intuitive

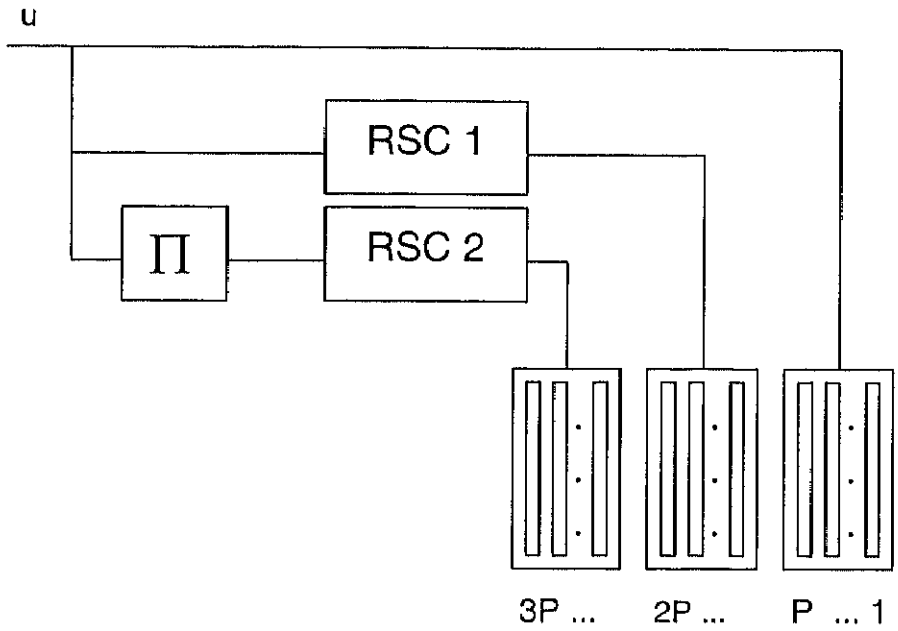

Figure 5.2: **Puncturing method for Turbo code**

idea for achieving UEP is to increase the number of redundancy symbols correlated with more important input symbols and to reduce the redundancy correlated with the less important symbols, while keeping the total redundancy constant.

Like RCPC codes, RCPT codes can be obtained when some restrictions are applied to the puncturing rule, i.e., the puncturing tables are selected so that all the Turbo codes with higher rates are realized by puncturing the different number of bits from the Turbo code with a lower rate. For RCPC codes, the puncturing tables are selected so that each successive transmission of the parity symbols yielded the greatest possible increment in the free distance of the new lower rate code. For RCPT codes, there are other more important criteria. In particular, the subsets of code symbols that have been transmitted at a given stage implicitly determine the number of MAP decoders that can be employed in receiver[62].

The RCPT encoder partitions the resulting code symbols in sub-blocks of (N/P) symbols, where P is the so-called puncturing period. In Figure 5.2, an example of the RCPT encoder is formed from an underlying rate 1/3 Turbo encoder with rate 1/2 RSC encoders. There are $3P$ total sub-blocks (each column) produced for potential transmissions. Each parity stream fills its matrix by row and is transmitted by column (like a block interleaver), i.e., the RCPT puncturing rule amounts to sending collections of one or more columns of the parity matrices so that at least P columns

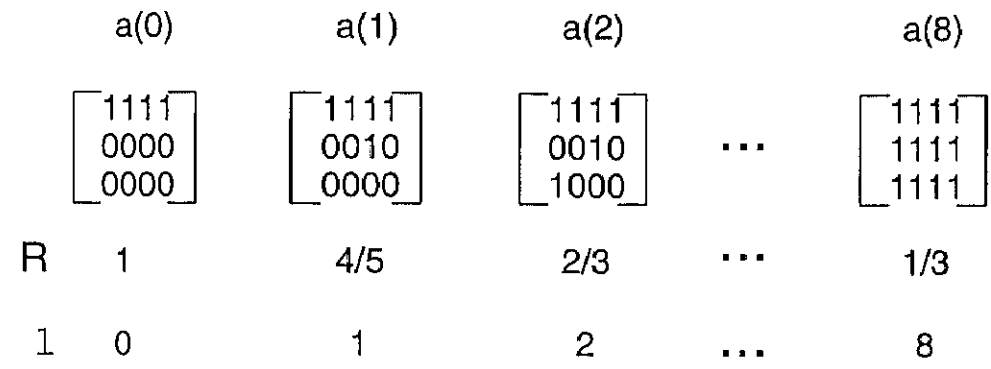

Figure 5.3: **Various puncturing matrices for Turbo code**

are sent in the transmission. The code construction allows for a family of codes of rates:

$$R_l = \frac{P}{P+l}, \qquad l = 0, 1, \cdots, 2P. \tag{5.6}$$

For each value of l, let a binary $3 \times P$ puncturing matrix be a(l). If $a_{ij} = 1$, then the j-th column of the i-th parity matrix belongs to the sub-code of rate R_l. Therefore, based on the above restrictions, a(0) must contain P or more ones, a($l+1$) must have ones in the same positions as in a(l) plus an additional one, and finally, a($2P$) has all ones.

As an example, an RCPT code with P=4 is formed from two rate 1/2 component RSC encoders. Then, the RCPT code can be any code rate in the set $\{1, \frac{4}{5}, \frac{2}{3}, \frac{4}{7}, \frac{1}{2}, \frac{4}{9}, \frac{2}{5}, \frac{4}{11}, \frac{1}{3}\}$ by selecting $4, 5, \cdots, 12$ columns from the parity matrices. The set of puncturing matrices could take the forms as shown in Figure 5.3, where all four columns of systematic bits (first row) are sent in the first packet a(0), the third column of the first encoder's non-systematic parity bits is sent in the second packet a(1), and the first column of the second encoder's non-systematic parity bits is sent in the third packet a(2). It is only after this third packet that the receiver can invoke the iterative encoder. From the above implementation, one need not utilize all possible code rates.

Because the capability to correct errors depends on the puncturing bit size, the redundancy symbols for the less important input symbols should be punctured more bits than the important ones. For two rate RCPT code, there are two puncturing matrices. However, the UEP cannot be achieved only by puncturing. Available interleavers are needed to provide a "support set invariance" property [63] that the permutation can map each support set onto the same set of positions in the interleaved frame. Then, the permutation matrix $\prod$ for a two rate Turbo code is described as

follows:

$$\prod = \sum \prod' \sum^T \tag{5.7}$$

where, ^{T} denotes transposing, $\prod'$ is a block diagonal permutation matrix with blocks of size $N_l \times N_l, (l = 1, 2)$, $\sum$ is the unique $K \times K$ permutation matrix that maps two support sets into the internals by keeping the position ordering in each support set and by ordering the support sets with decreasing class importance.

The $(N - t)$ encoder input symbols are partitioned into two importance classes S_H and S_P with sizes N_H and N_P, where they satisfy the following relation.

$$N_H + N_P = N - t. \tag{5.8}$$

In this way, a FEC scheme is obtained, where each class S_l of input symbols is locally protected by a PTC with rate R_l (l=1,2). Since t is generally much less than N_1 or N_2, these symbols can be included in the least important class S_2 with negligible information rate decrease. The overall rate R can be derived from the local rates R_H and R_P of the above encoding as below:

$$N_H/R_H + N_P/R_P = (N - t)/R. \tag{5.9}$$

In general, the $\frac{1}{R}$ is called as the bandwidth expansion factor of the FEC scheme.

According to the specific BER targets, RCPT codes with a desired level of UEP can be endowed by controlling a set of local rates, or assigning indices to each support set. Therefore, an application of variable PTCs allows the bandwidth efficiency to be exchanged with the reliability under the same hardware complexity.

5.3 Two Level UEP Scheme for Wireless ATM

In order to apply the two rate Turbo code to wireless ATM, an encoder input frame of wireless ATM cell is portioned into two importance classes S_H and S_P with sizes $N_H = 32$ bits (4 bytes) and $N_P = 384$ bits (48 bytes) corresponding to the header and payload[11]. Since the encoder starts and ends in the state zero for a MAP decoder, the information bits at the beginning and the end of a transmitted block have a lower bit error ratio [61]. Then, header bits are positioned at the beginning (first 16 bits) and the end (last 16 bits) of a frame, and the payload bits with the trellis termination t (equal to 4 bits when using 16 state component encoders) are positioned at the middle of the frame. The class position in an input frame is shown in Figure 5.4. The coding rates of the header bits and the payload bits are R_H and R_P, respectively. Let X_H and X_P be the sets of indices (support sets) of the header bits and the payload bits, respectively, which can be defined in below:

$X_H = \{1, 2, \ldots, 16, 401, 402, \ldots, 416\}$,

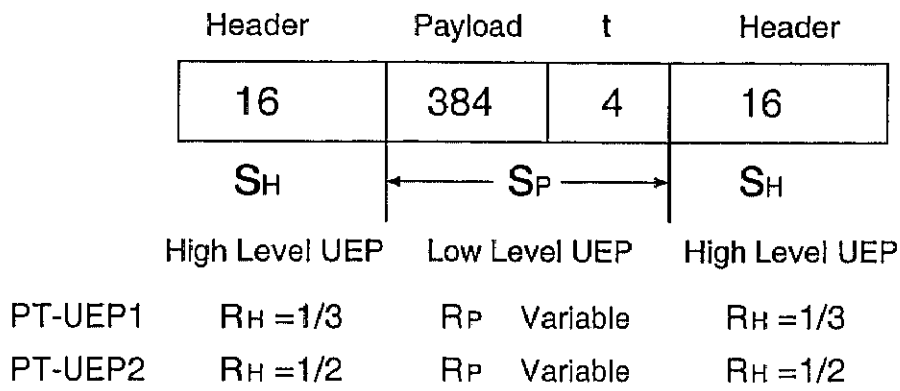

Figure 5.4: Input frame for two classes

$X_P = \{17, 18, \ldots, 400\}$.

As the total bits of the frame, N is expressed as :

$N = N_H + N_P + t = 32 + 384 + 4 = 420$.

Note that two different interleavers are required, i.e., one for S_H, another for S_P. As long as an interleaved sequence of information bits follows the same pattern (i.e., belongs to the same sequence) as a straight sequence of information bits, two outputs of the two interleavers can be connected in series. In order to be properly de-interleaved, the transmitted data are slit at the receiver end according to the sub-block they belong to.

Besides, an ATM payload is encoded for varying degrees of the error protection according to the required QoS. That is to say, for one VC, there is a corresponding FEC-H and FEC-P, which is adaptable to the different services. As shown in Figure 5.4, the following two schemes with different quality levels are considered. The PT-UEP1 scheme has $R_H = \frac{1}{3}$ Turbo codes for a header and various R_P Turbo codes for payloads. Its overall coding rate R becomes:

$$R = \frac{N - t}{N_H \times 3 + \frac{N_P}{R_P}} = \frac{32 + 384}{96 + \frac{384}{R_P}}. \tag{5.10}$$

For example, $R \doteq \frac{2}{3}$ when $R_P = \frac{3}{4}$.

The PT-UEP2 scheme has $R_H = \frac{1}{2}$ and various R_P, then the overall coding rate R becomes:

$$R = \frac{N - t}{N_H \times 2 + \frac{N_P}{R_P}} = \frac{32 + 384}{64 + \frac{384}{R_P}}. \tag{5.11}$$

For example, $R \doteq \frac{3}{4}$ when $R_P = \frac{4}{5}$.

For the Turbo code with rate $\frac{1}{3}$, puncturing is not needed. For Turbo codes with

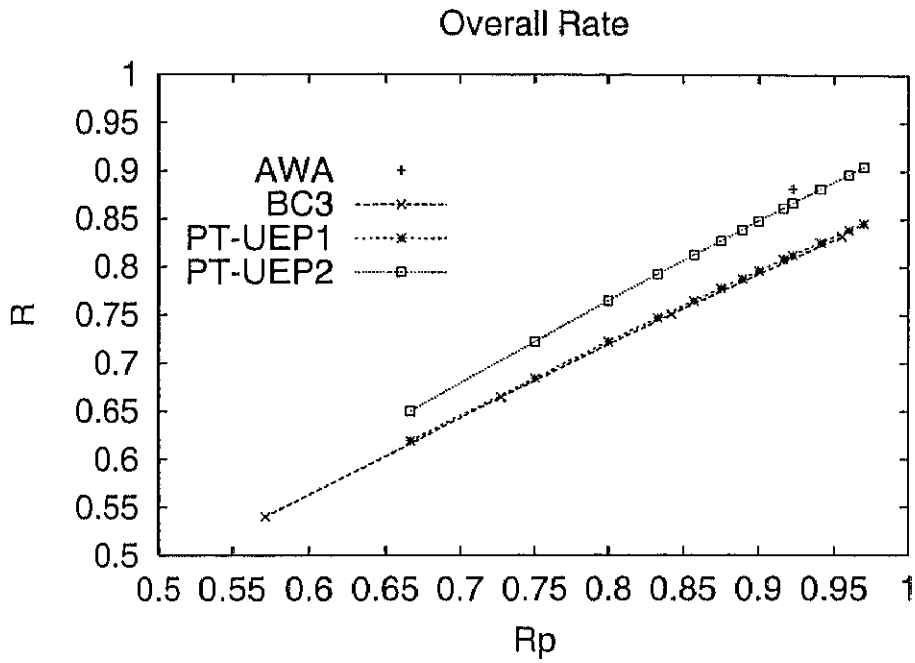

Figure 5.5: The values of overall rate of PT-UEP1 and PT-UEP2

rates $\frac{1}{2}, \frac{3}{4}, \frac{4}{5}$, the elementary puncturing matrices are selected as follows:

$$\begin{bmatrix} 1 & 0 \end{bmatrix}^T,$$

$$\begin{bmatrix} 1 & 0 & 0 & 0 & 0 & 0 \end{bmatrix}^T,$$

$$\begin{bmatrix} 1 & 0 & 0 & 0 & 0 & 0 & 0 & 0 \end{bmatrix}^T.$$

Obviously, through appropriate puncturing of the parity sequences, the Turbo codes having any rates are attainable. Since their perforation matrices is programmable, only one encoder circuit and one decoder circuit are needed for the various FEC-H and FEC-P even if their code rates, and thus the levels of error protection are different.

Figure 5.5 shows the relationships between R and R_P of PT-UEP1 and PT-UEP2, respectively. For comparison, the results of the previous BC3 and AWA schemes are cited. Suppose ARQ is not implemented at the DLC sublayer, i.e., for stream mode CBR/VBR services, the throughput of the DLC protocol is mainly influenced by the overall rate. Then from this figure, we know the PT-UEP1 scheme can achieve about the same throughput as the BC3 scheme, and the PT-UEP2 scheme can achieve the throughput of the AWA scheme when R_P becomes bigger.

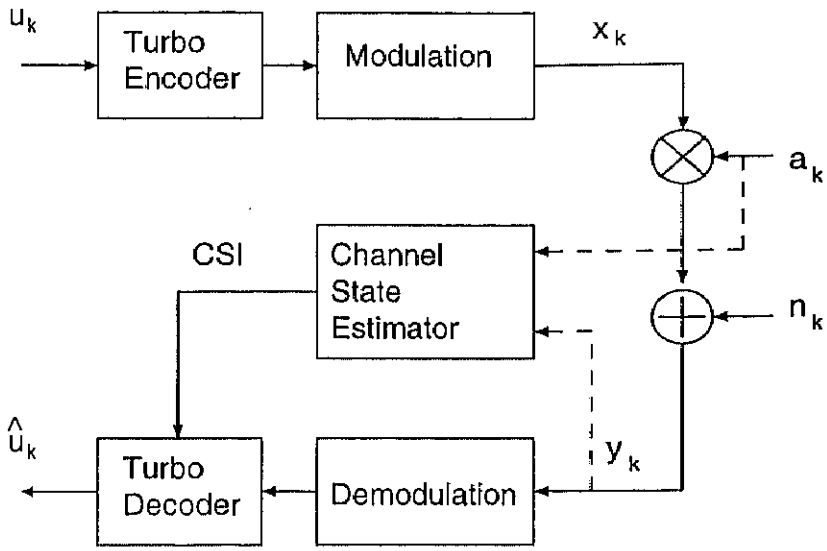

Figure 5.6: System simulation model over Rayleigh fading channel

5.4 Performance Analysis over Rayleigh Fading Channel

Rayleigh fading model represents the worst case model for the design engineer while offering analytical convenience as Chapter 4 mentioned. The model with a non-frequency-selective Rayleigh fading channel is shown in Figure 5.6. In this figure, u_k and $\hat{u}_k$ are the original and the decoded bits, respectively. After u_k is encoded and then modulated, x_k is obtained. y_k is the received data of x_k, described as follow:

$$y_k = a_k x_k + n_k, \tag{5.12}$$

where the fading amplitude a_k is a real Rayleigh-distributed random variable with $E(a_k^2)$=1 and n_k is the complex white Gaussian noise with one-sided power special density N_0. The full-interleaved fading channel is assumed, which means that a_k and y_k are statistically independent.

5.4.1 Bit Error Rate for UEP Turbo Code Scheme

The bit error rate of two level UEP schemes in Section 5.3 for wireless ATM is examined by simulation. The simulation in this section is proceeded for the PT-UEP1 scheme with $R_P = \frac{3}{4}$ and the PT-UEP2 scheme with $R_P = \frac{4}{5}$. These can be extended to the general cases. Without loss of generality, the component encoders are considered as two identical 16 (2^4) states and a half rate RSC encoder with the code generator (1, 21/37), which is both systematic for decoding simplicity and recursive to maximize the interleaver gain, as shown in Figure 5.7.

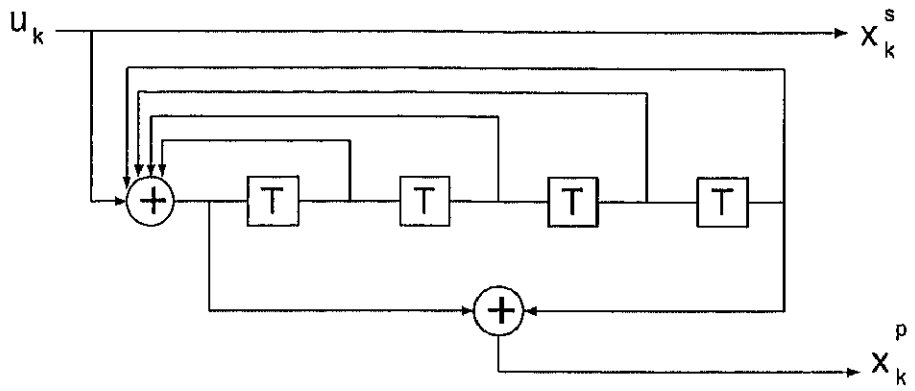

Figure 5.7: RSC encoder with the code generator (1, 21/37)

Decoding is implemented by the iterative decoder as described in Appendix B. A minimum of 1000 bit errors is counted for each simulated point. Here, a simple way is used to simulate puncturing, which is to set the received parity samples corresponding to the punctured parity bits to zero in the computation of log a posteriori probability (LAPP) ratio. Thus, the puncturing need not be performed at the encoder.

The BERs of PT-UEP1 and PT-UEP2 over Rayleigh fading channel as a function of bit position for a block with 420 bits are plotted in Figures 5.8 and 5.9, where SNR5, SNR6 and SNR7 represent the BER curves whose SNRs equal 5, 6 and 7 dB, respectively. These realize two level UEP with two kinds of interleaving and available puncturing. These figures show that the performance of the PTC is different from each other significantly if different puncturing matrix is employed. Then, the expected error probability can be achieved by changing them. Besides, there is no so-called "spill over" effect when switching from one rate to another, which means the transition between the two rate regions is very sharp.

5.4.2 Cell Loss Rate Bound Using Turbo Code

For CLR evaluation of UEP Turbo codes, it is sufficient to analyze the case that only a header is protected, since payload errors are not concerned from the definition of the CLR. Then, the analytic evaluation when the original Turbo code (EEP) is applied to header is discussed alone as below. When the $R = \frac{1}{3}$ Turbo code is applied to header, the probability of cell loss for coded systems is given by:

$$P_{coded} = 1 - (1 - P_{tc})^{32}, \tag{5.13}$$

where P_{tc} is the bit error probability of a wireless ATM header after using the Turbo code. Assuming a uniform interleaver and concerning the weight distribution of

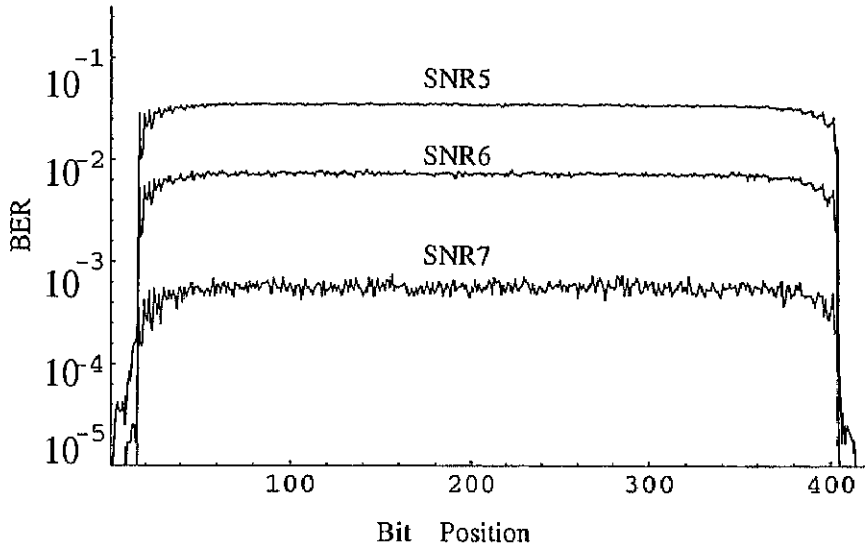

Figure 5.8: **The relationship between the BER of PT-UEP1 scheme and bit position for Rayleigh fading channel ($R = \frac{2}{3}$)**

codewords as [58], P_{tc} can be upper bounded by:

$$P_{tc} \leq \sum_{i=1}^{N} (\frac{i}{N})_N C_i E_{d/i}[P_2(d)], \tag{5.14}$$

where $E_{d/i}[.]$ is an expectation with respect to the distribution $p(d/i)$. $p(d/i)$ is the probability that an interleaving scheme maps an input weight i to produce a codeword with total weight d. $P_2(d)$ is the probability of choosing a specific wrong codeword differing from the correct codeword in d bit positions. For a full-interleaved Rayleigh fading channel with the CSI, it can be upper bounded by [64]:

$$P_2(d) \leq \frac{1}{2}[1 - (\frac{RE_b/N_0}{1 + RE_b/N_0})^{\frac{1}{2}}][\frac{1}{1 + RE_b/N_0}]^{d-1}. \tag{5.15}$$

For a full-interleaved Rayleigh fading channel without the CSI, it can be upper bounded by [64]:

$$P_2(d) \leq [e^{\frac{\gamma}{\beta}} \frac{\sqrt{1 + \frac{2}{\beta}} - 1}{\sqrt{1 + \frac{2}{\beta}} + 1}]^d, \tag{5.16}$$

where $\beta = \sqrt{\gamma^2 - 1}$ and $\gamma = RE_b/N_0$.

Figure 5.10 shows the CLR versus SNR analytic upper bound over the fully interleaved Rayleigh fading channel. In this figure, CSI and NSI are the results decoding with and without CSI, respectively. $R = \frac{1}{3}$ EEP Turbo code is used with the constraint length $K = 5$ of each component code, and $N = 420$ bits as before. For

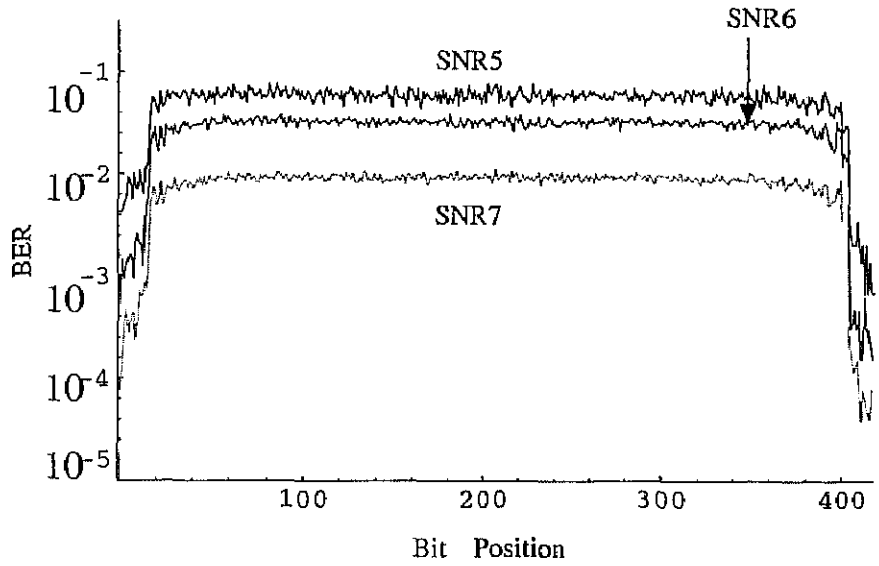

Figure 5.9: The relationship between the BER of PT-UEP2 scheme and bit position for Rayleigh fading channel ($R = \frac{3}{4}$)

reference, the uncoded scheme, HEC, AWA, BC3, PC-UEP4-s and PC-UEP4-h are added here, which are same as in Figure 4.19. Note that the BC3 and PC-UEP4 have the same coding rate as CSI and NSI. This shows that the SNR gains are still remarkably high for short frames (N=420 bits), and therefore the Turbo codes over header greatly decreases the degree of cell loss in theory. For example, Figure 5.10 indicates that the $R = \frac{1}{3}$ Turbo code using the BCJR decoding algorithm with CSI realizes 30 dB gain over the HEC, 16 dB gain over the AWA and 14 dB gain over BC3 at CLR of 10^{-4}.

It should be noted that the true performance of Turbo codes does not diverge at the low SNR as indicated by the bounds. In fact, the change in slope of the CLR bound curves around 10^{-5} is not the effect of channel, but rather an artifact of the union bound attributable to the over-counting. For the low SNR region, due to the divergence of the union bound, the analysis evaluation of Turbo codes is too difficult to be proven. Therefore, their performance must be examined based on simulation.

5.4.3 Cell Loss Rate for the UEP Turbo Code Scheme

In the simulation, wireless headers are treated separately from payloads, i.e., cells with errors at their headers are discarded but those with errors in the payloads are not, which is in line with the FEC schemes of Chapter 4.

Under the same simulation conditions as section 5.4.1, we have Figure 5.11, where

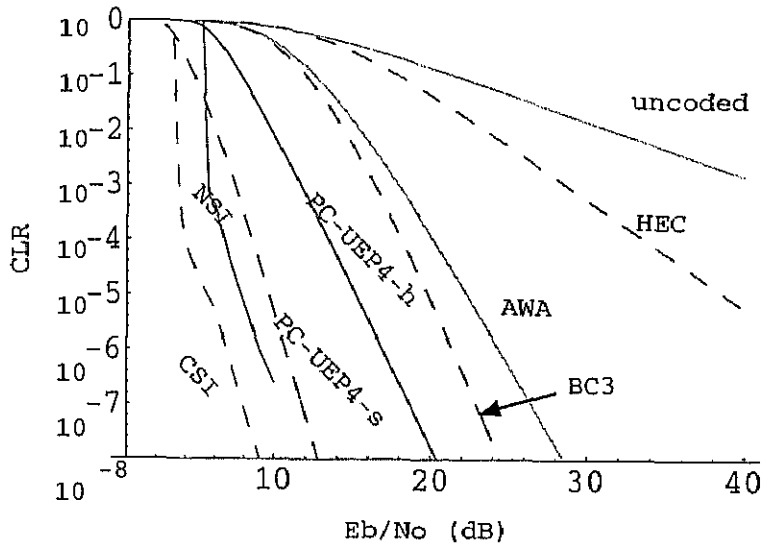

Figure 5.10: The CLR versus the SNR analytic upper bound over Rayleigh fading channel

the UEP Turbo code is compared with the EEP Turbo code with the same overall frame length $N = 420$ bits and about the same overall rates. This figure shows that the CLR versus E_b/N_0 for the UEP and EEP Turbo codes over the full-interleaved Rayleigh fading channel without CSI. There is a good agreement between the performance analysis and the simulation. For reference, AWA, BC3, PC-UEP2-h and PC-UEP4-h are added here. PT-EEP1 and PT-UEP1 have about the same total rate $R = \frac{2}{3}$, PT-EEP2 and PT-UEP2 have about the same total rate $R = \frac{3}{4}$. In order to make the comparison between the UEP and EEP Turbo codes independent from iterative decoding, the larger number of iterations, i.e., 20 is chosen. EEP is with a general random interleaver and uniform nonrandom puncturing[57]. Suppose CLR $\leq 10^{-3}$ (i.e. PCS applications) is required, PT-UEP1 without CSI meets these conditions at $E_b/N_0 = 4.4$ dB, while the PT-EEP1 code without CSI needs $E_b/N_0 = 7.6$ dB. So, the coding gain of the PT-UEP1 with respect to the PT-EEP1 is 3.2 dB.

5.4.4 Balance between Header CLR and Various Payload BER

The relationship between the CLR and the payload BER over fully interleaved Rayleigh fading channel is shown in Figure 5.12, where three solid lines represent BC3, AWA and HEC, and two dashed lines are PT-UEP1 and PT-UEP2, respectively. BC3 denotes (49,16) 6-bit error-correcting block code for a header and (402,384) 2-bit error correcting block code for a payload. HEC denotes the scheme only applying HEC to

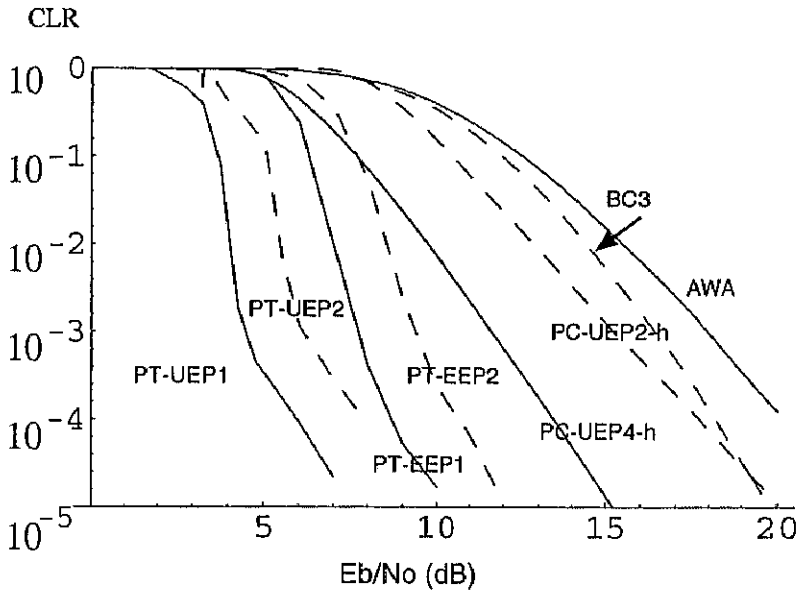

Figure 5.11: The CLR versus SNR for the UEP and the EEP Turbo codes over Rayleigh fading channel without CSI

the header. Obviously, PT-UEP1 and PT-UEP2 have as good balance performance as the BC3 and AWA, respectively.

Within the higher BER region, the reason that PT-UEP1 and PT-UEP2 are far from HEC is that the RCPT codes for header is more efficient than those for payload. On the other hand, when BER becomes lower, the reason that PT-UEP1 and PT-UEP2 have the trends diverging from HEC is the difference between the error correcting abilities of RCPT codes for header and payload becomes smaller.

5.5 Discussions

Turbo codes have some delay due to the utilization of the interleaver. The interleaver size is given by the number of bits to be sent in the specified time, which is dependent on both the allowable delay time and the transmission bit rate. In order to be able to apply Turbo code to the time-sensitive services, the small interleaver size (N=420 bits) is utilized for small delay. The analysis has shown that improvements are attainable even for this short interleavers.

For the time-insensitive services with properties of smaller CLR and allowable delay, the larger interleaver size (e.g., the multiples of 420 bits) should be available, due to the common belief that Turbo codes work better with large interleavers. From the viewpoint of the transmission delay, data services can tolerate a larger delay

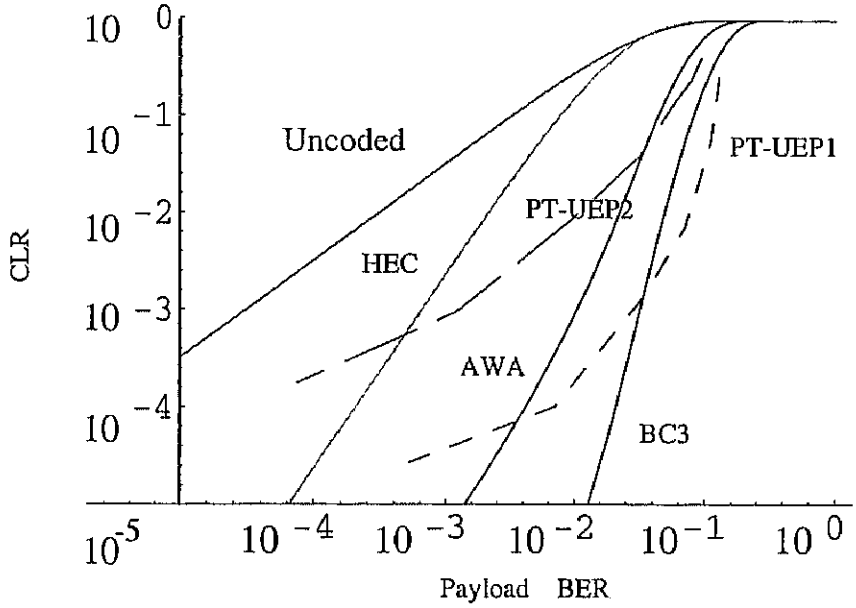

Figure 5.12: **Balance characteristics for PT-UEP1 and PT-UEP2**

compared with voice services in general, and result in a larger interleaver size too. Because of these reasons, Turbo codes are more effective in data transmission services.

In addition, because wireless communication systems have high error rates in general, CLR may be improved by reducing packet length[28]. But this is not suitable for the FEC scheme using RCPT codes [16], due to the performance of Turbo codes largely depending on their input block length.